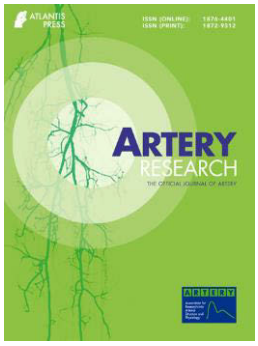

Artery Research

ISSN (Online): 1876-4401 **ISSN (Print): 1872-9312**
Journal Home Page: https://www.atlantis-press.com/journals/artres

P120: A MODEL-BASED STUDY ON THE EVOLUTION OF BLOOD PRESSURE DURING AGEING

Stamatia Pagoulatou, Nikolaos Stergiopulos

To cite this article: Stamatia Pagoulatou, Nikolaos Stergiopulos (2017) P120: A MODEL-BASED STUDY ON THE EVOLUTION OF BLOOD PRESSURE DURING AGEING, Artery Research 20:C, 77–78, DOI: https://doi.org/10.1016/j.artres.2017.10.102

To link to this article: https://doi.org/10.1016/j.artres.2017.10.102

Published online: 7 December 2019

As a consequence of the local deceleration, the detachment of the boundary layer from the wall develops a disturbed flow, which impacts hemodynamics. It results in a non-uniform distribution of wall shear stress (WSS), which is responsible for atherosclerosis [1]. This phenomenon usually occurs in the carotid bifurcation (CB). Computational methods, MRI and conventional Doppler techniques have been used to establish the correlations between flow disturbance and plaque formation. We propose the use of a new method, called high-frame rate Vector Flow imaging (VFI), which dynamically visualises blood flow velocities in all directions, in the evaluation of the flow characteristics in the CB [2,3,4,5].

Methods: CB geometries and flow patterns in 30 healthy subjects of different age were evaluated using a commercial system equipped with high-frame rate VFI based on a frame rate of 600 Hz. The flow is represented by many coloured vectors, displayed as arrows, showing the different velocity, magnitude and direction at each site.

Results: The correlation between flow disturbances and carotid sinus diameter was confirmed: the more relevant the diameter, the more disturbed the flow. Different CB geometries, affecting the flow behaviours and generating complex flow, such as recirculation, counter eddy, vortex and helical trajectory, were identified (Fig 1).

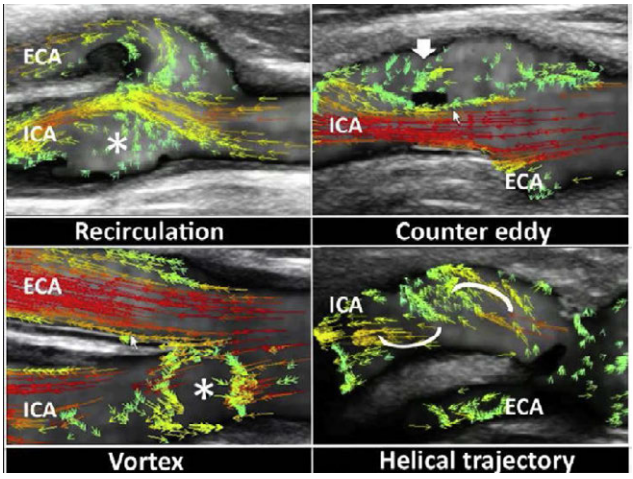

Conclusions: High-frame rate VFI shows in detail the spatiotemporal characteristics of the flow and demonstrates the strong effect of vessel geometries on the flow patterns.

References

1. Younis HF, Kaazempur-Mofrad MR, Chan RC et al. Hemodynamics and wall mechanics in human carotid bifurcation and its consequences for atherogenesis: investigation of inter-individual variation. Biomech Model Mechanobiol 2004; 3:17—32
2. Yiu BY, Lai SS, Yu AC. Vector Projectile Imaging: Time-Resolved Dynamic Visualization of Complex Flow Patterns. Ultrasound Med Biol 2014; 40(9):2295—2309
3. Du Y, Fan R, Li Y. Ultrasonic imaging method and system. WO2015180069A1, 2015 4. Goddi A. Fanizza M, Bortolotto C et al. Vector Flow Imaging techniques — A new way to study vessel flow with ultrasound. JCU 2017. Jul 21. DOI:10.1002/jcu.22519 [Epub ahead of print] 5. Goddi A, Bortolotto C, Fiorina I et al. High-frame rate vector flow imaging of the carotid bifurcation. Insights Imaging 2017;8:319.

P85

HIGH FRAME RATE DYNAMIC DISPLAY ULTRASOUND VECTOR FLOW IMAGING FOR QUANTITATIVE STUDIES OF HEMODYNAMICS OF CAROTID ARTERIES

Yigang Du [1], Xujin He [1], Yingying Shen [1], Lei Zhu [1], Alfredo Goddi [2]
[1]*Shenzhen Mindray Bio-Medical Electronics Co. Ltd., Shenzhen, China*
[2]*Centro Medico SME-Diagnostica per Immagini, Varese, Italy*

Advanced atherosclerotic patients are faced with significant risks of stroke, which are very likely to cause death or irreversible physical disability. However, the growth of artery stenosis usually needs a very long development. Early diagnosis is necessary and requires detailed and accurate quantitative hemodynamics to be supported. The paper proposes an angle-independent ultrasound flow imaging technique for carotid arteries, which allows true velocity vectors measurement, obtaining both value and direction of blood flow.

The proposed vector flow imaging is implemented based on multi-directional Doppler interleaved transmission [1,2], with high frame rate dynamic display [1] and zone sonography technology [3].

Hemodynamics becomes extremely complicated when plaques develop in the carotid bulb. The dynamic display with velocity vectors assesses flow patterns, e.g. laminar flow, vortex and turbulence (Examples are shown in the figure). The circular variance for the angles of vectors in a desired region of interest can be calculated, allowing disturbance quantification for the non-laminar flow. The method is capable of measuring volume flow (VF) and wall shear stress (WSS) at different locations. To ensure the accuracy both VF and WSS are calculated based on a frame rate of 400—600 Hz and vector velocities.

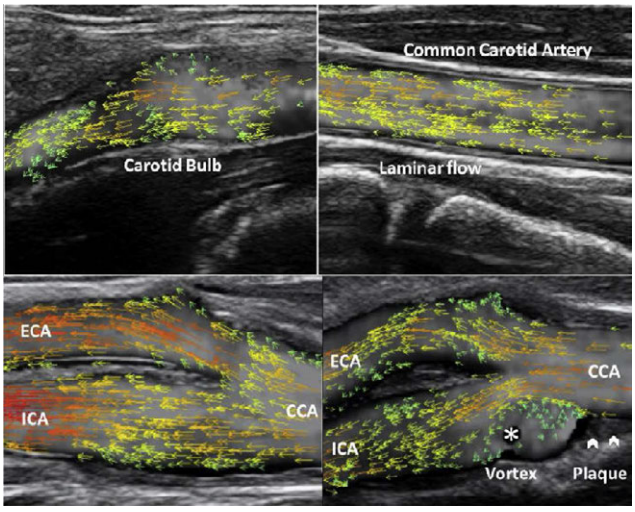

The high frame rate vector flow imaging has been implemented in a commercial ultrasound system. It provides various quantitative results such as circular variance, VF and WSS, which are useful for hemodynamics studies of complex flow. This could make the early prevention and diagnosis of carotid disease possible.

References

[1] Yiu B Y S, Lai S S M, Yu A C H. Vector projectile imaging: Time-resolved dynamic visualization of complex flow patterns. Ultrasound in Medicine and Biology, 2014; 40(9): 2295—2309.
[2] Du Y, Fan R, Li Y. Ultrasonic imaging method and system. 2015, WO2015180069A1
[3] Napolitano D J, Debusschere B D, Mclaughlin G W, et al. Continuous transmit focusing method and apparatus for ultrasound imaging system. 2011, US8002705B1

Poster Session 1 — Models and Methodologies I

P120

A MODEL-BASED STUDY ON THE EVOLUTION OF BLOOD PRESSURE DURING AGEING

Stamatia Pagoulatou, Nikolaos Stergiopulos
Laboratory of Hemodynamics and Cardiovascular Technology, EPFL, Switzerland

Background: Hypertension being a major risk factor of cardiovascular mortality, there is a pressing need to understand the ageing mechanisms that lead to the continuous increase of pulse pressure and systolic blood pressure over time. Alterations in both forward and backward waves with age have been widely recognized as key features affecting the development of

hypertension, with investigators, however, not reaching a consensus on the relative importance of each wave component (1,2).
Objective: The aim of the current investigation was to examine the wave profile over time after developing an age-adapted, mathematical, one-dimensional model of the cardiovascular system.
Methods: Our state-of-the-art 1-D model (3,4) was extended to include turbulence and inertial effects of the flow exiting the left ventricle. Literature data on the age-associated changes in arterial stiffness, peripheral resistance and cardiac contractility were gathered and used as an input for the simulation.
Results: The predicted evolution of pressure and augmentation index with age followed accurately the curves obtained in a number of large-scale clinical studies. Analysis of the relative contribution of the forward and backward wave components showed that the forward wave becomes the major determinant of the increase in central and peripheral SBP and PP with advancing age.
Conclusions: The 1-D model of the ageing tree and heart captures faithfully and with great accuracy the central pressure evolution with ageing. The stiffening of the proximal aorta and the resulting augmentation of the forward pressure wave is the major contributor of the systolic pressure augmentation with age.

References
1. O'Rourke MF, Nichols WW. Changes in Wave Reflection With Advancing Age in Normal Subjects. Hypertension. 2004 Dec 1;44(6):E10—1.
2. Mitchell GF, Conlin PR, Dunlap ME, Lacourcière Y, Arnold JMO, Ogilvie RI, et al. Aortic diameter, wall stiffness, and wave reflection in systolic hypertension. Hypertens Dallas Tex 1979. 2008 Jan;51(1):105—11.
3. Reymond P, Bohraus Y, Perren F, Lazeyras F, Stergiopulos N. Validation of a patient-specific one-dimensional model of the systemic arterial tree. Am J Physiol Heart Circ Physiol. 2011 Sep; 301(3):H1173- 1182.
4. Reymond P, Merenda F, Perren F, Rüfenacht D, Stergiopulos N. Validation of a one-dimensional model of the systemic arterial tree. Am J Physiol — Heart Circ Physiol. 2009 Jul 1;297(1):H208—22.

P121
IDENTIFYING HAEMODYNAMIC DETERMINANTS OF PULSE PRESSURE: AN INTEGRATED NUMERICAL AND PHYSIOLOGICAL APPROACH

Samuel Vennin, Ye Li, Marie Willemet, Henry Fok, Haotian Gu, Peter Charlton, Jordi Alastruey, Phil Chowienczyk
King's College London, UK

Purpose: Hypertension, the single biggest killer worldwide[1], arises mainly as a result of an increase in central pulse pressure (PP)[2], yet haemodynamic basis of that increase is still disputed. We examined the ability of a simple "reduced" model comprising a proximal characteristic impedance linked to a Windkessel element to accurately predict PP from aortic blood flow and applied the model to examine PP dependence on cardiac and vascular properties.
Method: PP obtained from the model was compared with theoretical values obtained in silico and in vivo. Theoretical values were obtained using a distributed multi-segment model in a population of "virtual" subjects (n = 3,095) in which cardiovascular properties were varied over the pathophysiological range. In vivo measurements were in normotensive subject (n = 13) during modulation of physiology with vasoactive drugs with divergent actions on cardiac and cascular properties and in hypertensive subjects (n = 156).
Results: PP derived from the model agreed with theoretical values (mean difference SD, -0.09 ± 1.96 mmHg) and with measured values (-1.95 ± 3.74 and -1.18 ± 3.67 mmHg for normotensive and hypertensive subjects respectively). Parameters extracted from the model agreed closely with theoretical and measured physical properties. PP was seen to be determined mainly by total arterial compliance (inversely associated with arterial stiffness) and ventricular dynamics: the volume of blood ejected up to time of pulse pressure and the rate of ventricular ejection up to this point.
Conclusion: Increased flow and/or volume accounted for 20.1 mmHg (52%) of the 39.0 mmHg difference in pulse pressure between the upper and lower tertiles of the hypertensive subjects.

References
1. Lim SS, Vos T, Flaxman AD, et al. A comparative risk assessment of burden of disease and injury attributable to 67 risk factors and risk factor clusters in 21 regions, 1990—2010: A systematic analysis for the global burden of disease study 2010. Lancet. 2012;380:2224-2260
2. Franklin SS, Gustin W, Wong ND, Larson MG, Weber MA, Kannel WB, Levy D. Hemodynamic patterns of age-related changes in blood pressure. The framingham heart study. Circulation. 1997;96:308-315

P122
CALCULATING RESERVOIR PRESSURE WITH OR WITHOUT FLOW INFORMATION: SIMILARITY AND ALGORITHMIC SENSITIVITY AT RADIAL ARTERY

Michael Ebner [1], Kim Parker [2], Tom Vercauteren [3,1], Sébastien Ourselin [3,1], Siegfried Wassertheurer [4], Alun Hughes [5], Bernhard Hametner [4]
[1]*Translational Imaging Group, Centre for Medical Image Computing, Department of Medical Physics and Biomedical Engineering, University College London, London, UK*
[2]*Department of Bioengineering, Imperial College London, London, UK*
[3]*Wellcome / EPSRC Centre for Interventional and Surgical Sciences, University College London, London, UK*
[4]*Center for Health & Bioresources, AIT Austrian Institute of Technology, Vienna, Austria*
[5]*Institute of Cardiovascular Science, University College London, London, UK*

Background: Reservoir pressure is typically estimated from the pressure waveform information only. Comparability with estimates made using pressure and flow depend on assumptions, e.g. a proportional relationship between excess pressure and flow [1]. In this study, we compared (i) results using flow and pressure versus pressure-only at the radial artery, and (ii) two different algorithms used in the literature for pressure- only analysis.
Methods: Reservoir pressure separations were performed on 95 hypertensive individuals where radial pressure and flow velocity waveform measurements were available [2]. Algorithm (F) used flow and pressure information [3]. Algorithms (P1) and (P2) refer to the two different pressure-only implementations as used in [4, 5], and [1, 6], respectively. Reservoir curves characterized by physiologically implausible parameters, i.e. a rate constant $b < 0$ or an asymptotic pressure $P_\infty < 0$, were discarded, leaving 63 subjects with valid reservoir pressure data.
Results: Estimated reservoir parameters are shown in Table 1. Algorithm (F) showed statistically significant differences in most of the parameters compared to (P1) and (P2), although, except time constant τ and asymptotic pressure P_∞, there was a strong correlation between methods. Significant differences were observed in reservoir pulse pressure and area estimates between (P1) and (P2) despite their, in general, high correlation.

Table 1. Quantification of reservoir pressures p_{res} obtained by methods (F), (P1) and (P2) at radial artery in the format of mean $\pm$ standard deviation based on 63 subjects whereby PP denotes the reservoir pulse pressure, A_p the area of reservoir pressure above diastolic blood pressure, τ the time constant describing the diastolic pressure decay, P_∞ the asymptotic blood pressure and $a,b = 1/\tau$ the rate constants. Peripheral (area) resistance and compliance, i.e. R and C, were estimated from the rate constants a and b for (P1) and (P2) using flow information. The correlation coefficient r was computed between relevant methods. The statistical significance of the differences between methods was based on a paired t-test with * indicating $p < 0.05$.

Radial artery	p_{res} (F)	p_{res} (P1)	p_{res} (P2)	r(F,P1)	r(F,P2)	r(P1,P2)
PP [mmHg]	41.5 ± 10.0	36.3 ± 7.2	35.7 ± 7.0	0.82*	0.82*	0.96*
A_p [mmHg s]	17.5 ± 4.3	15.6 ± 3.7	15.5 ± 3.7	0.94*	0.94*	1.00*
τ [S]	0.3 ± 0.1	0.6 ± 0.4	0.6 ± 0.3	0.36*	0.42*	0.88
P_∞ [mmHg]	65.7 ± 10.3	63.9 ± 15.2	64.8 ± 12.6	0.45	0.53	0.79
a [1/s]	—	8.1 ± 5.2	7.4 ± 2.7	—	—	0.93
b [1/s]	—	2.2 ± 1.1	2.1 ± 0.8	—	—	0.84
R [mmHg s/m]	419.0 ± 188.8	453.7 ± 348.2	436.7 ± 302.6	0.68	0.75	0.92
C [mm/mmHg]	0.8 ± 0.3	1.7 ± 1.0	1.7 ± 1.0	0.70*	0.70*	1.00